Adaptive Camber Variation Utilising Local Anisotropy

by U.-C. EHLERT, P. GÜNTHER, A. BÜTER, D. SACHAU, and E. BREITBACH

German Aerospace Center
Institute of Structural Mechanics
Lilienthalplatz 7, D-38108 Braunschweig
Germany

1. Abstract

This paper presents an investigation of an actively controllable camber variation for rotor blades. The new structural concept described here is based upon a 3-cell blade design using tension-torsion-coupling together with piezoelectric stack-actuators to bend the cross-section about the blade axis. A finite-element-model of an adaptive camber rotor blade is used to perform a parameter optimisation to maximise camber variation at the blade tip. Both, geometric as well as material and manufacturing parameters are evaluated. Their influence is presented.

2. Introduction

Active control of the aerodynamic shape of rotor blades is the key to enhance helicopter flight envelopes and at the same time reduce noise emission as well as vibrational passenger disturbance. This control capability is also essential to improve wind energy converter energy output and endurance.

In contrast to the active twist concepts that have already been thoroughly investigated /1, 2, 3/ the adaptive camber concept allows active *shape* control for rotor blades. Furthermore, no flaps or other moving parts are used so that the aerodynamic surface in the deformed state is expected to remain smooth without any gaps, edges, or dents.

2.1 Approach

Prior to a detailed investigation of the aerodynamic effects of an adaptive camber variation first the exact shape of the deformed rotor blade is to be evaluated. The aim is to validate the expected surface quality of the deformed rotor blade and to collect the necessary data about the change of geometry that is required for the subsequent aerodynamic calculations.

3. Structural Concept

The adaptive camber rotor blade has a three-cell cross-section that consists of carbon-glass-fibre composites supported by structural foam.

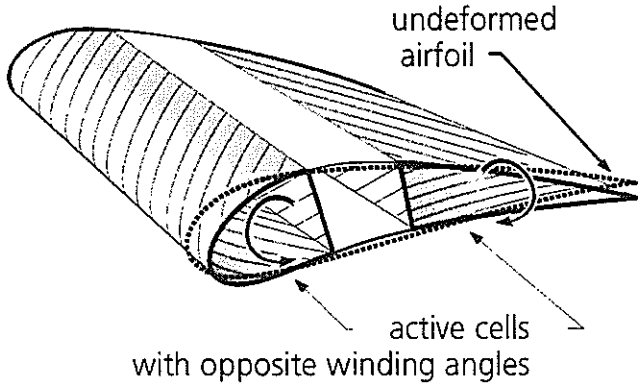

Figure 1 Principle of the Adaptive Camber Variation

The desired change of camber is achieved using tension-torsion-coupling in the outer cells that are activated by piezo-electric stack-actuators integrated into the blade tip.

Manufacturing these active cells with helical windings at opposite fibre angles leads to simultaneous upward or downward movements of the blade's edges, as shown in Fig. 1. The resulting continuous change of the rotor blade's camber steadily increases from zero at the root to it's maximum at the tip.

4. Finite-Element-Model

The structural concept was investigated using a three-dimensional parametric model designed in the commercial finite-element code ANSYS® 5.3 (see Fig. 2). Aerodynamic as well as structural loads were not considered in the design of this model, since only the deformed airfoil's surface quality was of interest here. For the same reason, neither spars nor ribs were represented in the model rotor blade.

Both shell elements and solid elements were used in this model. The element size was chosen to have the airfoil shape represented with at least 100 nodes.

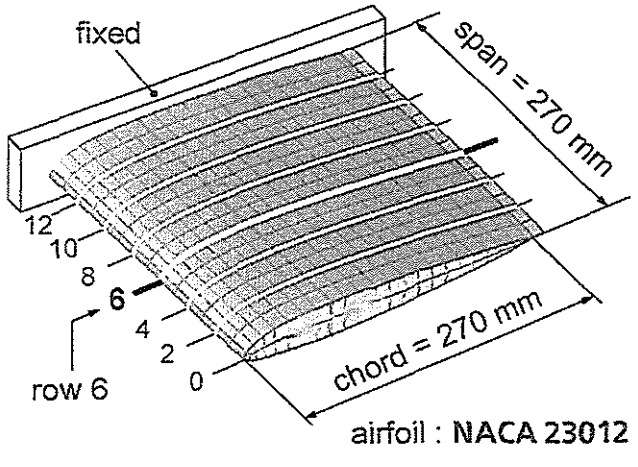

Figure 2 Finite Element Discretisation

4.1 Geometry

The model's chord was set to 270 mm corresponding to the MBB BO 105 rotor blade. The blade model was fixed at its root and activated by an elongation of 0.5 mm at it's tip. The span was set to 270 mm, so that the singularities at the model's boundaries did not significantly influence the middle section of the model. In this section (element row 6, as shown in Fig. 2) the resulting change of camber was evaluated.

This parametric model was programmed to be applied to different airfoils. The results presented in this paper were calculated for the MBB BO 105 airfoil, the NACA 23012.

4.2 Materials used

The structural concept described above comprises three different materials: Carbon-fibre-composite, glass-fibre-composite and structural foam.

The carbon-fibre-composite was used in the helical winding layers of both active cells to realise the desired tension-torsion-coupling. This composite consists of HM carbon fibre and epoxy resin with 60% fibre volume fraction.

The outer skin of the model consists of glass-fibre-composite made from glass fabric (100 g/m²) oriented at 45°. Resin material and fibre volume fraction were assumed to be the same as in the carbon-fibre composite.

Foam cores were used in each of the three cells to support the fibre layers and to guarantee the desired airfoil's shape.

The manufacturing process of a rotor blade equipped with active camber variation was supposed to begin with the active cells. First the helical carbon-fibre unidirectional (UD) layers were attached to the foam cores. Next the two outer cells were connected to the middle cell's foam core. Last the glass-fibre layers were attached as the outer skin in order to finish the rotor blade.

This process is not suitable for the design of a real rotor blade including structural and aerodynamic loads. Yet it is feasible for the proof-of-principle demonstration structure, that will

be required later to experimentally validate the expected deformation properties of this concept.

The proposed manufacturing process determined the composite lay-up for the model, as it is shown in Fig. 3 for the model's cross-section.

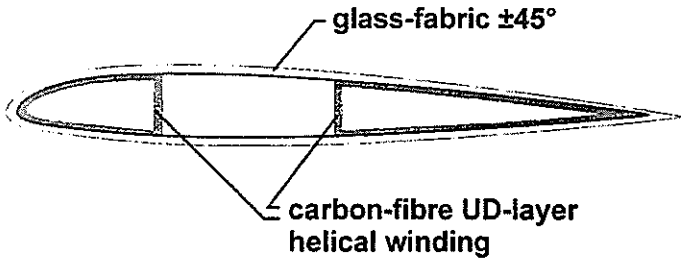

Figure 3 Composite Lay-up

4.3 Parameters

Geometric as well as material parameters were considered in the evaluation of the adaptive camber concept described above.

Three groups of parameters were evaluated:

- the positions of the inner cell walls,
- the fibre angles of the carbon-layers, and
- the thickness of carbon- and glass-layers.

The inner cell walls' positions were given in percent chord, ranging from 15 % to 70 % for the front wall and from 35 % to 85 % for the rear wall. These parameter boundaries were arbitrarily chosen in order to allow for a wide range of possible cell wall position combinations. Furthermore, the rear wall was locally restricted, so that it was always positioned behind the front wall. This precaution was necessary for the subsequent automatic parameter optimisation. The increment was set to 5 for both walls to keep the number of wall position combinations small.

The fibre orientation of the carbon-fibre layers ranged from 0° to 45° in the leading edge cell and from –45° to 0° in the trailing edge cell. An angular increment of 5° was chosen for both cells due to restrictions in manufacturing precision. The active cells' orientation angles were independend of each other.

The thickness of the carbon- and glass-fibre layers varied from 0.2 to 5 mm for each layer with a 0.2 mm increment according to manufacturing accuracy.

These seven parameters (2 wall positions , 2 fibre angles, 3 thicknesses) were investigated in the following calculations to gather information over the parameters' influence on the maximum camber variation.

4.4 Evaluation

In each of the subsequent calculations a different set of parameter values was evaluated concerning the maximum change of camber, the rearward position of this maximum, and the angle of attack at element row 6 (as illustrated in Fig. 2). These data were extracted from nodal positions and displacements within each program run and stored for later evaluation.

The change of camber was calculated from the difference between the mean lines of the undeformed and the deformed rotor blade model. Therefore, the mean lines had to be extracted from model data in each program run.

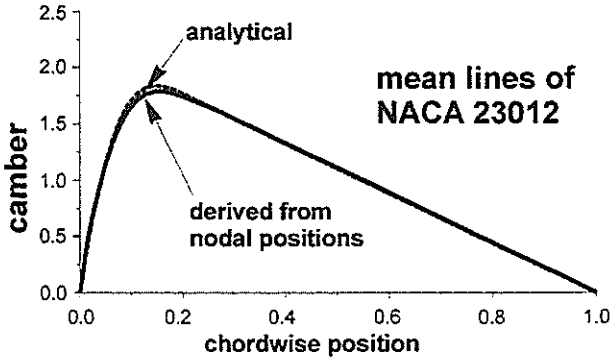

Figure 4 Comparison of Mean Lines

To prove the feasibility of this approach, the mean line of the NACA 23012 was derived from the nodal positions in the FE-model and compared to the mean line calculated from the analytical formula. The maximum difference

was less than 0.1 % of the analytical mean line. This accuracy was sufficient for the subsequent parameter investigations.

The difference between undeformed and deformed airfoil camber gave the change of camber.

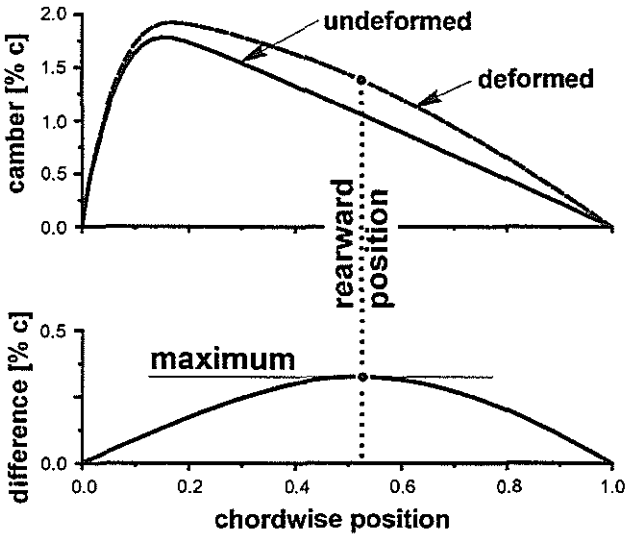

Figure 5 Change of Camber

For the final evaluation of this change of camber only its maximum and the rearward position of this maximum were used, see Fig. 5.

Since both leading edge and trailing edge of the airfoil change their position when the camber variation is activated, an influence on the angle of attack was expected. For this reason, the angle of attack was derived from the displacements of the leading and trailing edge nodes prior to the evaluation of the change of camber. Afterwards, the coordinate system was rotated to compensate for the calculated blade twist before the change of camber was evaluated. In this way, the two degrees of freedom camber variation and blade twist could be investigated separately.

5. Influence of Parameters

In order to evaluate the influence of the parameters, each group of parameters was investigated separately with the other parameters set to fixed values.

5.1 Wall Positions

For this investigation layer thicknesses were set to 0.8 mm for both carbon-fibre layers and to 0.2 mm for the glass-fabric layer, respectively. Fibre angles of 20° for the leading edge cell and -20° for the trailing edge cell were used.

The **overall maximum change of camber** reached **0.33 % chord**, it was achieved for the front cell wall at 35 % chord and the rear cell wall at 55 % chord (white cross in Fig. 6). The camber change of the other wall position combinations is presented in relation to this global maximum, i.e. 1.00 in the contour plot equals the camber variation of 0.33 % chord.

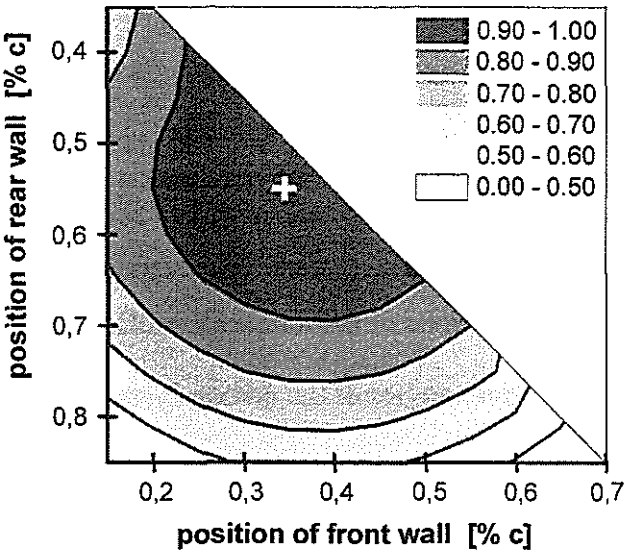

Figure 6 Maximum Change of Camber

The overall maximum is comparatively flat, so that 90 % of this maximum can be obtained in a wide range of wall position combinations (front cell wall between 25 % and 45 % or rear cell wall between 45 % and 65 %). Therefore, no further restrictions had to be imposed on manufacturing procedures with regard to the precision of cell wall positioning.

The rearward position of the maximum change of camber is given in percent chord, see Fig. 7. For most wall position combinations the maximum lies beyond 50 % chord. In order to place this maximum closer to the

leading edge and at the same time obtain at least 90 % of the global maximum change of camber, it is possible to use a wall position combination of 25 % (front) and 45 % (rear).

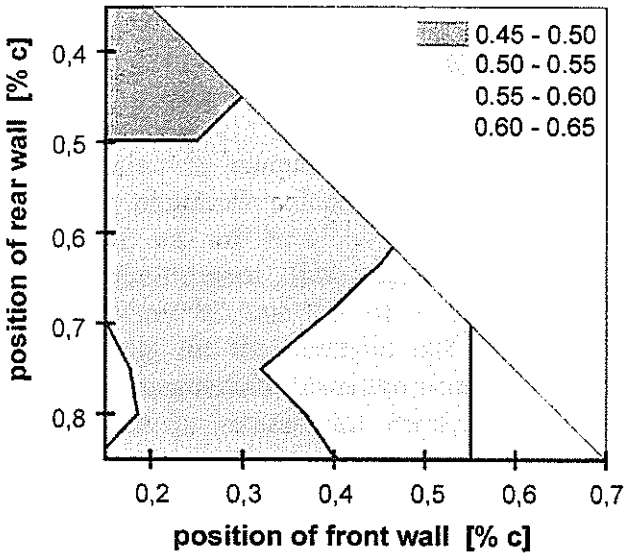

Figure 7 Rearward Position of Maximum

The change of angle of attack α is given in Fig. 8. The unit of α is

$$[\alpha] = (\tan\alpha)\cdot 1000 \ .$$

The maximum positiv angle of attack (represented as 10.0 in Fig. 8) reached 0.573°.

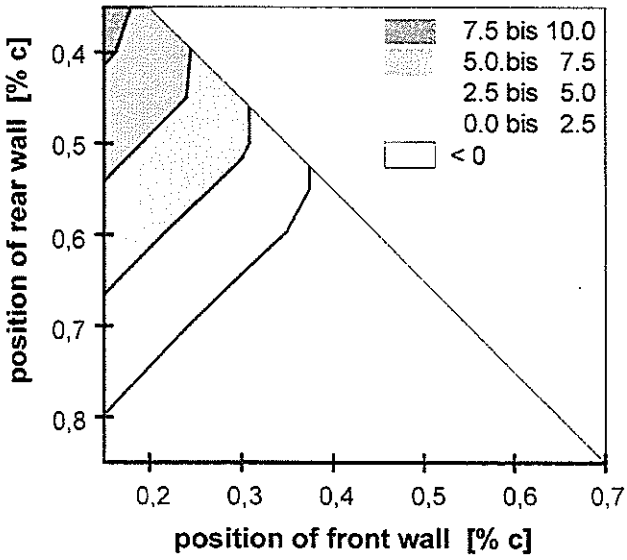

Figure 8 Change of Angle of Attack

Negativ angles of attack were also observed, but they were not investigated further, since they corresponded directly to the most rearward positions of camber change maximum.

Figures 9 and 10 give an impression of the deformation of the NACA 23012 airfoil with different cell wall position. In both figures the upper sketch illustrates the entire deformation (camber and twist), the lower sketch shows the change of camber only. The vertical displacements are multiplied by a factor of 50 in order to make the deformation visible.

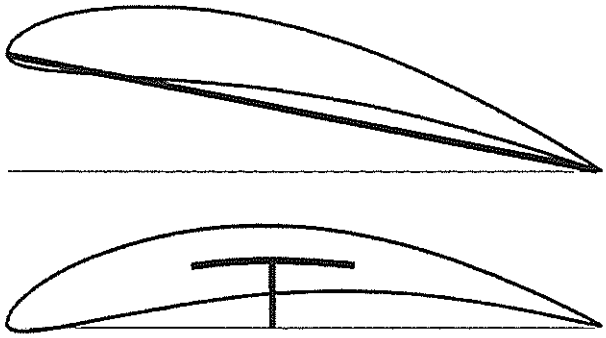

Figure 9 Walls at 15 % and 45 %

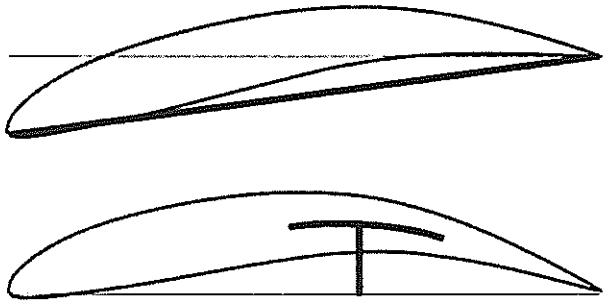

Figure 10 Walls at 50 % and 70 %

5.2 Fibre Angles

For the investigation of the fibre angles' influence on the adaptive camber, cell walls were set to 30 % and 50 %. The layer thicknesses were set to 0.8 mm for both carbon-fibre layers and to 0.2 mm for the glass-fabric layer.

The **overall maximum change of camber** reached **0.32 % chord**, it was obtained for carbon layer fibre angles –15° in the trailing edge cell and 20° in the leading edge cell. The contours in Fig. 11 are given in rela-

tion to this maximum, so that 1.00 represents the global maximum of change of camber. 90 % of this maximum could be obtained from a wide range of fibre angle combinations, so that fibre angles will not be critical manufacturing parameters.

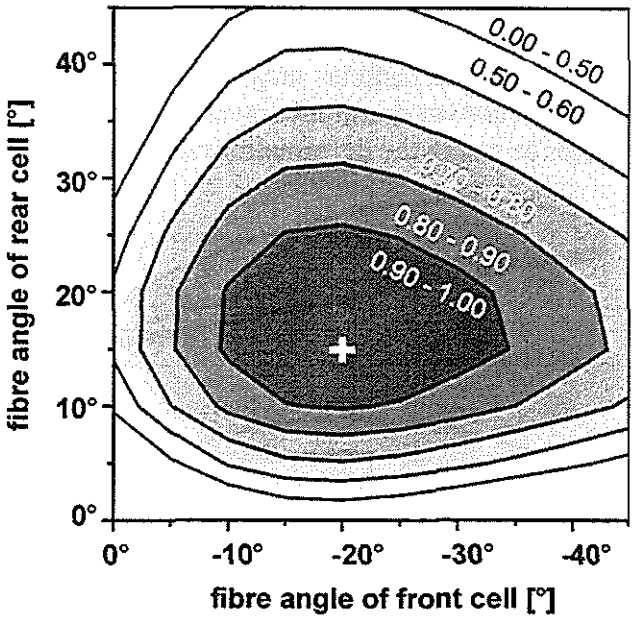

Figure 11 Maximum Change of Camber

The rearward position of the maximum was strongly dominated by the cell wall positions, so that fibre angle combinations showed hardly any influence.

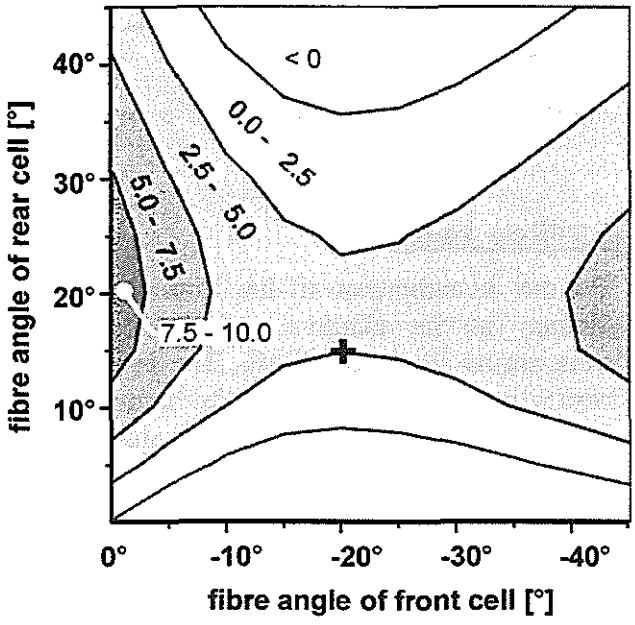

Figure 12 Change of Angle of Attack

The angles of attack reached 0.29° in the vicinity of the global maximum of the change of camber. Maximum angles of attack were achieved for front cell fibre angles close to 0°, that are not suitable to maximise the change of camber.

5.3 Layer Thicknesses

To investigate the influence of carbon-layer thicknesses on the camber variation, wall positions were set to 30 % for the front and 50 % for the rear wall, respectively. Fibre angles were set to –20° and 20° for front and rear cell. The thickness of the glass-fabric layer (0.2 mm) remained unchanged. In a first step, only layer thicknesses up to 2.0 mm were used.

The **overall maximum change of camber** reached **0.39 % chord**, it was obtained for carbon layer thicknesses 2.0 mm in the trailing edge cell and 2.0 mm in the leading edge cell. Fig. 13 illustrates, that best results were achieved with equal layer thicknesses in both cells.

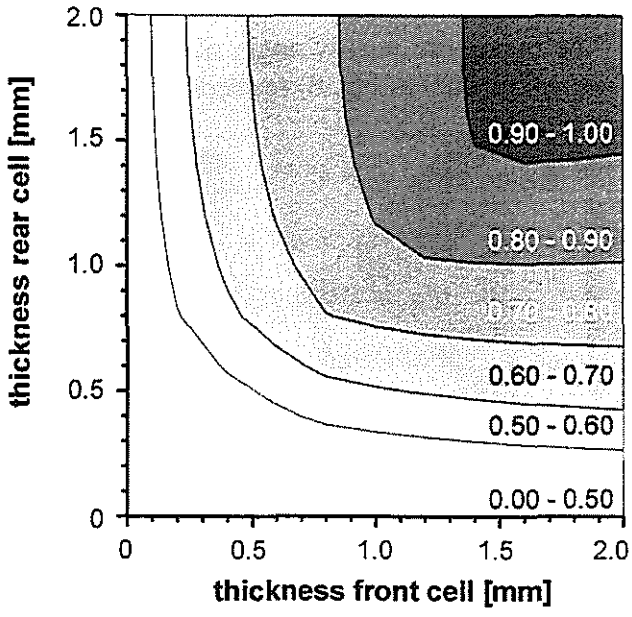

Figure 13 Maximum Change of Camber

With layer thicknesses beyond 1.5 mm 90% of the global maximum could always be obtained. Thus, basic manufacturing precision

will be sufficient to build a demonstration rotor blade with adaptive camber variation.

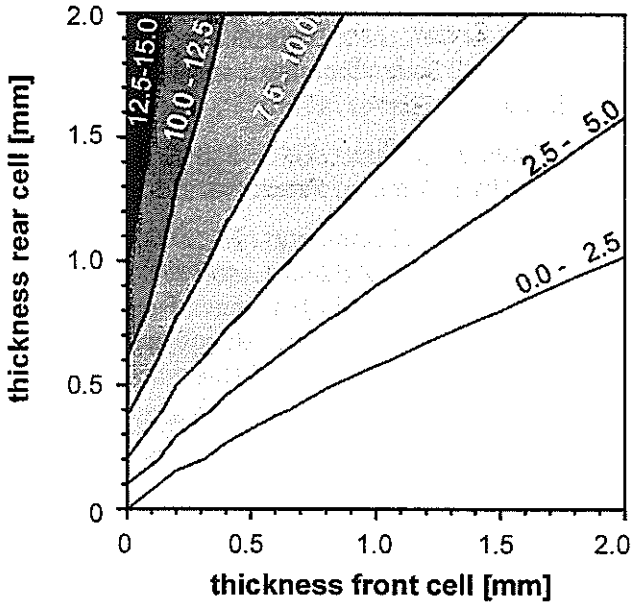

Figure 14 Change of Angle of Attack

Angles of attack reach 0.3° near the maximum of change of camber. High angles only occured with front cell wall thickness near 0.0 mm, that are not suitable (see above).

In a second step, layer thicknesses beyond 2.0 mm were investigated.

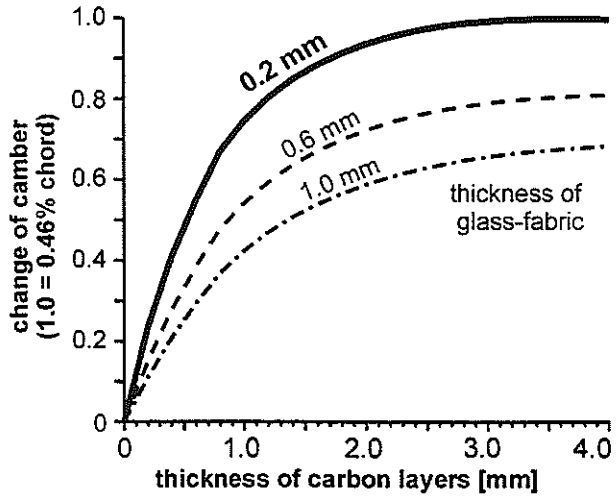

Figure 14 Thickness of Glass-fabric

Fig. 14 illustrates the effects of equally thick carbon-layers in front and rear cell. Furthermore, the influence of the glass-layer's thickness is given.

Walls thicker than 2.0 mm do not show significant gain in change of camber. On the other hand they bring additional weight and cause increasing manufacturing problems especially near the trailing edge. Therefore, carbon-layer thickness should not exceed 2.0 mm.

The glass-fabric's thickness limits the maximum of change of camber, so that this layer should be as thin as possible. Since thin layers are difficult to manufacture the glass-layer thickness should be at least 0.2 mm.

All three parameter groups proved to have similarly great influence on the camber variation. Therefore, it was necessary to identify the combination of parameters, that yielded the largest change of camber.

5.4 Optimisation

Using the automatic optimisation capabilities of the FE-program, a parameter optimisation was performed. The thickness of the glass-fabric layer was set to 0.2 mm, all other parameters were free for variation.

The resulting angles of attack were restricted to positive values, the rearward position of the maximum change of camber was constrained not to exceed 60% chord.

Under these conditions the maximum change of camber reached 0.547% chord. This was obtained from the following parameter combination :

front cell wall at 35% chord

rear cell wall at 55% chord

front carbon fibre orientation –20°

rear carbon fibre orientation 20°

carbon fibre thickness 2.0 mm

The maximum's rearward position was 52,5% chord, the angle of attack was less than 0.01°.

To further increase the change of camber, it would be necessary to allow rearward positions beyond 60% chord and to accept negative angles of attack. This decision has to be

taken carefully with respect to the aerodynamic effects of such an airfoil variation.

6. Conclusions and Outlook

A structural concept of the adaptive camber variation for helicopter and wind turbine rotor blades was investigated. The decisive structural parameters were identified, their influence on the change of camber and the angle of attack was described. The concept proved to have the expected surface qualities in the deformed state.

Steps to be taken include the consideration of thin airfoils (9% and less) to increase the maximum change of camber. Next a demonstration structure is to be designed and manufactured. The goal is to experimentally validate the deformation qualities and to investigate the dynamic properties and deformation quantities. As soon as the aerodynamic requirements are investigated another demonstration structure can be designed and manufactured taking into account the static and dynamic structural and aerodynamic loads.

7. Acknowledgements

The authors gratefully acknowledge the support of essential parts of the research work presented in this paper by the *DEUTSCHE BUNDESSTIFTUNG UMWELT*.

8. References

1. Büter, A. : *INVESTIGATION OF ADAPTIVE CONCEPTS FOR VIBRATION REDUCTION, NOISE SUPPRESSION AND IMPROVED AERODYNAMIC EFFICIENCY* ; Doctoral Thesis, RWTH Aachen, Germany, 1998
2. Chopra, I. : *DEVELOPMENT OF A SMART ROTOR* ; 19th European Rotorcraft Forum, Cernobbio (Como), Italy, 1993
3. Hagood, N.W. and Derham, R.C. : *ROTOR DESIGN USING SMART MATERIALS TO ACTIVELY TWIST BLADES* ; American Helicopter Society 52nd Annual Forum, Washington D.C., 1996
4. Barrett, R. and Brozoski, F. : *ADAPTIVE FLIGHT CONTROL SURFACES, WINGS, ROTORS AND ACTIVE AERODYNAMICS* ; SPIE Symposium on Smart Structures and Materials, San Diego, California, 1996
5. Büter, A. , Ehlert, U.-C. and Breitbach, E. : *PROFILE* , German Patent No. 198 04 308.2
6. Geissler, W. , Sobieczky, H. : *DYNAMIC STALL CONTROL BY VARIABLE AIRFOIL CAMBER* ; AGARD 75th Fluid Dynamics Panel Meeting and Symposium on Aerodynamics and Aeroacoustics of Rotorcraft, Berlin, 1993
7. Strehlow, H. and Rapp, H. : *SMART MATERIALS FOR HELICOPTER ROTOR ACTIVE CONTROL* ; AGARD/SMP Specialists Meeting on Smart Structures for Aircraft and Spacecraft, Lindau, Germany, 1992